PERGAMON

International Journal of Heat and Mass Transfer 41 (1998) 3611–3625

International Journal of HEAT and MASS TRANSFER

An efficient simulation of the heat and mass transfer processes during drying of capillary porous, hygroscopic materials

Christian Dietl[a,*], Edgar R. F. Winter[a], Raymond Viskanta[b]

[a]*Technische Universität München, Lehrstuhl C für Thermodynamik, Munich, Germany*
[b]*Purdue University, School of Mechanical Engineering, USA*

Received 19 February 1996; in final form 6 November 1997

Abstract

The optimization of drying processes as well as the design of drying equipment can be accomplished by computer simulation. In order to predict the drying behavior of capillary porous, hygroscopic materials a numerical model simulating the convective heat and mass transfer and an efficient method in determining the coefficients for the moisture conductivity and the vapor diffusion resistance by an inverse procedure are introduced. For demonstrating the efficacy of the simulation model as well as the inverse procedure the theoretical predictions of the simulation model derived for steady and time dependent drying conditions are compared with experimental data.

Nomenclature

a_w water activity
A area [m^2]
c specific heat [$J(kg\ K)^{-1}$]
h heat enthalpy [$J\ kg^{-1}$]
H enthalpy [J]
$\dot{H}$ enthalpy flow rate [$J\ s^{-1}$]
m mass [kg]
$\dot{m}$ mass flow rate [$kg\ s^{-1}$]
$\dot{n}$ mass flux [$kg(m^2\ s)^{-1}$]
p pressure [Pa]
p_v^* saturated vapor pressure [Pa]
$\dot{q}$ heat flux [$W\ m^{-2}$]
$\dot{Q}$ heat flow rate [W]
r particle coordinate [m]
R_v gas constant for vapor [$J\ (kg\ K)^{-1}$]
t time [s]
T absolute temperature [K]
w velocity [$m\ s^{-1}$]
U inner energy [J]
V volume [m^3]
x_a absolute air humidity [$kg\ kg^{-1}$]
X moisture content (substance) [$kg\ kg^{-1}$].

Greek symbols

α heat transfer coefficient [$W\ (m^2\ K)^{-1}$]
α^* corrected heat transfer coefficient [$W\ (m^2\ K)^{-1}$]
β mass transfer coefficient [$m\ s^{-1}$]
δ vapor diffusivity [$m^2\ s^{-1}$]
Δr space step [m]
Δt time step [s]
ϑ relative temperature [°C]
κ moisture conductivity [$m^2\ s^{-1}$]
λ thermal conductivity [$W\ m\ K^{-1}$]
μ vapor diffusion resistance
ϱ density [$kg\ m^{-3}$]
φ relative air humidity.

Subscripts

a drying medium air
f fluid, liquid
l element
r location
R at the surface
sx moist substance
sdr dry substance

* Corresponding author.

0017–9310/98 $19.00
PII: S0017–9310(97)00357–8

t time
v vapor
w water.

1. Introduction

The paper introduces an efficient computational tool for predicting the convective drying behavior of capillary porous, hygroscopic materials. This ability in forecasting the drying behavior is an important prerequisite for the prompt and cost efficient optimization of drying processes. Criteria supporting such an optimization are the enhancement of product quality, better process control, more efficient use of the drying equipment and the reduction in primary energy utilization.

The starting point for the development of a numerical model describing the drying behavior of single solids was an extensive literature review [1] and the known principles of heat and mass transfer. The single solid model forms a basis for the development of an additional model simulating packed bed drying. Special attention was given to the validation of both models not only for steady but also for time dependent drying conditions. With respect to packed bed drying, the fact that the drying conditions for single solids at different depths within the packed bed change with time due to the moisture increase of the drying fluid while flowing the bed cannot be ignored.

In order to predict the relatively complex drying processes only known or easy to determine input parameters are considered for the derivation of the model equations. With the exception of the coefficients for the moisture conductivity and the vapor diffusion resistance, the equations for all state properties, states of equilibrium and transport properties used in the numerical model are obtained in the literature. By definition, the moisture conductivity and the vapor diffusion resistance are closely linked to the single solid model, meaning that their values cannot simply be taken from the available literature. Moreover, the effort in experimentally determining the two transport coefficients does not justify the means by which this is accomplished. Therefore an inverse procedure is developed to enable the determination of the two a priori unknown coefficients with the help of experimentally determined drying curves.

A foundation for the optimization of drying processes is based on the derivation and verification of the model equations for drying of single solids and the development of an inverse procedure to determine the two unknown transport coefficients. The following discussion illustrates the modeling of single solid drying and the implementation of the inverse procedure. The modeling of packed bed drying is described in the dissertation [1] and will be published in a separate paper.

2. Physical–mathematical and numerical model

2.1. Derivation of the model equations

The single solid model is based on the heat and enthalpy as well as mass balances in the liquid and vapor states for a differential control volume. Geometries considered are those of a sphere, cylinder and flat plate. For these geometries the differential control volume is defined as $\Delta V_r = A_r \cdot \Delta r$, where A_r represents the control surface and Δr the thickness at any given location r. In order to compute the transport processes it was necessary to reduce the three-dimensional problem into a quasi one-dimensional one. This is accomplished by only considering heat, enthalpy and mass flows perpendicular to the control surface. The energy and mass balance provides a set of partial differential equations for the moisture content and temperature of the product. These model equations can be solved numerically if all relevant transport properties are known.

2.1.1. Energy balance

The following assumptions are made for the heat transfer processes in the material: air flow in the pores triggered by vapor motion as well as thermal diffusion are neglected. Likewise, heat generation within the substance—for example, by chemical reaction—is disregarded. As shown in subsequent consideration moisture transfer contributions in the liquid and vapor phase are described separately.

Therefore, the energy transfer in the substance to be dried results from the heat flow rate $\dot{Q}_\lambda$ due to thermal conduction and the enthalpy flow rates $\dot{H}_\mathrm{f}$ and $\dot{H}_\mathrm{v}$ of the liquid and vapor initiated by moisture transfer. Balancing of the heat and enthalpy flow rates $\dot{Q}_\lambda$, $\dot{H}_\mathrm{f}$ and $\dot{H}_\mathrm{v}$ and taking the converted binding enthalpy $\Delta\dot{H}_\mathrm{B}$ per unit time into account, leads to the time rate of change of the internal energy $\partial\Delta U/\partial t$ for the differential control volume. Expanding the transport terms in Taylor series and disregarding higher order terms, the energy equation becomes

$$\frac{\partial \Delta U}{\partial t} = -\frac{\partial \dot{Q}_\lambda}{\partial r}\Delta r - \frac{\partial \dot{H}_\mathrm{f}}{\partial r}\Delta r - \frac{\partial \dot{H}_\mathrm{v}}{\partial r}\Delta r - \Delta\dot{H}_\mathrm{B}. \tag{1}$$

The following relations are valid for the terms given in equation (1):

Fourier–Biot Law describes the heat conduction in the substance depending on the thermal conductivity $\lambda(X, \vartheta)$ which is a function of the moisture content $X := (m_\mathrm{w}/m_{sdr})$ and temperature ϑ,

$$\dot{Q}_\lambda = -\lambda A_r \frac{\partial \vartheta}{\partial r}. \tag{2}$$

Heat convection in the liquid and vapor states, respectively, is dependent on the specific enthalpy of the liquid and vapor transferred with the mass flux,

$$\dot{H}_f = \dot{m}_f h_f, \quad \dot{H}_v = \dot{m}_v h_v. \tag{3}$$

According to Luikov [2], the heat convection in the liquid is negligible compared to the convection of heat in the vapor. In other words, the term $\partial \dot{H}_f/\partial r$ can be neglected.

It should be noted that in addition to the enthalpy of evaporation $h_v(\vartheta)$ already included in the enthalpy balance, the binding enthalpy $h_B(X)$ must be considered in describing the change of state of the product moisture. Krischer and Kast [3] provide an equation for the binding enthalpy utilizing the mathematical relationship for sorption isotherms,

$$h_B(X) = -R_v \frac{\mathrm{d}(\ln a_w)}{\mathrm{d}\left(\frac{1}{T}\right)}. \tag{4}$$

The required binding enthalpy $\Delta \dot{H}_B$ per unit time is defined as

$$\Delta \dot{H}_B = \frac{\partial}{\partial t}(\Delta m_v h_B) = \frac{\partial \dot{m}_v h_B}{\partial r}\Delta r. \tag{5}$$

The mass of the moist substance to be dried is given by $\Delta m_{sx} = \varrho_{sdr} A_r X \Delta r$. Furthermore, it is assumed that the product moisture defined as the ratio of mass of moist product and mass of dry product is present as a liquid. This simplification is necessary since a more detailed analysis of the product moisture regarding its state of aggregation introduces an additional property, namely the porosity of the product, which further restricts the applicability of the model. Hence, the change of the internal energy for the differential control volume is given by

$$\frac{\partial \Delta U}{\partial t} = \frac{\partial}{\partial t}(\Delta m_{sx} h_w + \Delta m_{sdr} h_{sdr}) = \varrho_{sdr} A_r (c_{sdr} + X c_w)\frac{\partial \vartheta}{\partial t}. \tag{6}$$

Substituting the above mentioned relationships into equation (1) and eliminating of Δr leads to the partial differential equation for the temperature $\vartheta(r, t)$ of the drying material as a function of the location r and time t,

$$\varrho_{sdr} A_r (c_{sdr} + X c_w)\frac{\partial \vartheta}{\partial t} = -\frac{\partial \dot{Q}_\lambda}{\partial r} - \frac{\partial \dot{m}_v (h_v + h_B)}{\partial r}. \tag{7}$$

Combining equation (7) with the relationships for heat conduction $\dot{Q}_\lambda$ [equation (2)] and mass transfer in the vapor state $\dot{m}_v$ [equations (10) and (12) derived in the next section] results in

$$\varrho_{sdr} A_r (c_{sdr} + X c_w)\frac{\partial \vartheta}{\partial t} = \frac{\partial}{\partial r}\left(\lambda A_r \frac{\partial \vartheta}{\partial r}\right) + \frac{\partial}{\partial r}\left(\frac{\delta}{\mu} A_r \frac{p_v^*}{R_v T}\left(\frac{\partial a_w}{\partial X}\right)\frac{\partial X}{\partial r}(h_v + h_B)\right). \tag{8}$$

Now, the change per unit time of the internal energy and, therefore, the change of the product temperature can be computed.

2.1.2. Mass balance

Two separate terms are required to describe the mass transfer for hygroscopic and nonhygroscopic moisture contents within the substance. Due to the lack of a partial vapor pressure gradient the transfer of non-hygroscopic moisture takes place exclusively in a liquid or absorbed state, for example, initiated by surface phenomena.

Balancing of the inflow and outflow mass flow rates for the control volume $\Delta V_r = A_r \cdot \Delta r$ yields the change in moisture of the drying substance $\partial \Delta m_{sx}/\partial t$ per unit time. Again use of the Taylor series, while neglecting higher order terms, leads to the mass balance equation,

$$\frac{\partial \Delta m_{sx}}{\partial t} = -\frac{\partial \dot{m}_f}{\partial r}\Delta r - \frac{\partial \dot{m}_v}{\partial r}\Delta r. \tag{9}$$

The terms contained in this equation are described by the following relations:

The mass of the moist product Δm_{sx} in the differential control volume is expressed in terms of the moisture content X,

$$\Delta m_{sx} = \varrho_{sdr} A_r X \Delta r.$$

The mass transfer rate in the vapor state m_v for atmospheric drying is usually determined by applying Fick's law which is analogous to Fourier–Biot Law of heat conduction. The driving force is the vapor pressure gradient and vapor mass flow rate can be expressed as

$$\dot{m}_v = -A \frac{\delta(\vartheta)}{\mu}\frac{1}{R_v T}\frac{\partial p_v}{\partial r}. \tag{10}$$

The vapor pressure gradient develops within the material to be dried which is already greatly dehumidified results in air filled pores whose geometry barely changes with further dehumidification and which enhance the diffusion process. If in addition, it is assumed that the pores impose an almost constant resistance to the diffusion flux as compared to the free diffusion of water vapor in air, then, the vapor diffusion coefficient $\delta(\vartheta)$ can be substituted by the temperature dependent diffusion coefficient of the solvent in the drying medium (in this case water vapor in air) and the vapor diffusion resistance μ can be approximated as a constant.

For the mass transfer rate in the liquid state m_f Krischer [3] recommends an approach analogous to Fick's law with the moisture gradient as the driving force,

$$\dot{m}_f = -A\kappa(X, \vartheta)\varrho_{sdr}\frac{\partial X}{\partial r}. \tag{11}$$

Nevertheless, it has to be kept in mind that the transport coefficient used in equation (11)—the moisture diffusivity $\kappa(X, \vartheta)$—is a function of temperature, moisture content and the substance itself as opposed to the vapor diffusion coefficient $\delta(\vartheta)$ in equation (10) which is only a function of temperature.

Studies by Jokisch [4] indicate that mass transfer in the vapor and in the liquid states are linked in such a way that for every vapor pressure in the pore space the corresponding sorption equilibrium is achieved. According to Krischer and Kast [3], this occurs very rapidly. If the moisture content under equilibrium conditions is known as a function of the water activity a_w and temperature ϑ of the product—in other words if the sorption behavior of the drying material is known—use of the expression

$$p_v = a_w(X,\vartheta)\cdot p_v^*(\vartheta)$$

allows the relationship between the partial vapor pressure gradient $\partial p_v/\partial r$ and the moisture gradient $\partial X/\partial r$ to be stated as

$$\frac{\partial p_v}{\partial r} = \frac{\partial p_v}{\partial X}\cdot\frac{\partial X}{\partial r} + \frac{\partial p_v}{\partial \vartheta}\cdot\frac{\partial \vartheta}{\partial r}.$$

In the case of convective drying maximum temperature gradients for the cross section of the substance are only present at the beginning of the drying process and since the corresponding high moisture contents minimize the partial differential of the water activity a_w the above equation can be simplified to

$$\frac{\partial p_v}{\partial r} = \frac{\partial p_v}{\partial X}\cdot\frac{\partial X}{\partial r} = p_v^*\left(\frac{\partial a_w}{\partial X}\right)\frac{\partial X}{\partial r}. \tag{12}$$

This relationship leads to an equation for the total mass flow rate with the moisture gradient as the driving potential

$$\begin{aligned}\dot m &= \dot m_f + \dot m_v \\ &= -[A_r(\kappa(X,\vartheta)\varrho_{sdr})]\frac{\partial X}{\partial r} \\ &\quad -\left[A_r\left(\frac{\delta(\vartheta)}{\mu}\frac{p_v^*}{R_vT}\left(\frac{\partial a_w}{\partial X}\right)\right)\right]\frac{\partial X}{\partial r}.\end{aligned} \tag{13}$$

Substituting of the above mentioned relationships into the mass conservation equation (9) leads to the partial differential equation for the moisture $X(r,t)$ of the drying material

$$\varrho_{sdr}A_r\frac{\partial X}{\partial t} = \frac{\partial}{\partial r}\left[A_r\left(\kappa\varrho_{sdr} + \frac{\delta}{\mu}\frac{p_v^*}{R_vT}\left(\frac{\partial a_w}{\partial X}\right)\right)\frac{\partial X}{\partial r}\right]. \tag{14}$$

The model equation enables the calculation of the change of product moisture with the help of the expressions for the local changes of the mass flow rate in the liquid and vapor phases.

2.1.3. Boundary conditions

At $t = 0$ the initial conditions are the temperature profile and the moisture profile of the substance being dried. Also, the state of the product is dependent on the preceding process step and the nature of the product itself. Some agricultural substances, for example, display extreme moisture gradients and for this reason the initial conditions have to be carefully considered. Usually, however, constant temperature and moisture profiles can be assumed at the beginning of a drying process.

The boundary conditions in the middle of the product are derived from the symmetry condition. Here, a temperature gradient as well as a moisture gradient is absent meaning that the heat and moisture flow rates at the location $r = 0$ vanish at any given time t,

$$\dot Q_\lambda|_{r=0,t} = \dot m_v|_{r=0,t} = \dot m_f|_{r=0,t} = 0. \tag{15}$$

At the product surface $r = R$, the known relationships for heat transfer $\dot Q_\alpha$ and mass transfer $\dot m_\beta$ are valid,

$$\dot Q|_{r=R,t} = -\dot Q_\alpha = -\alpha^* A_R(\vartheta_a - \vartheta_R), \tag{16}$$

$$\dot m_v|_{r=R,t} = \dot m_\beta = \beta A_R\frac{p}{R_vT}\ln\frac{p-p_{vl}}{p-p_{v,R}},$$

$$\dot m_f|_{r=R,t} = 0. \tag{17}$$

2.2. Determination of the transport coefficients

The transport coefficients contained in the model equations for heat and mass transfer in the product are: (1) the heat and mass transfer coefficients α and β, (2) the thermal conductivity λ, (3) the moisture conductivity κ, (4) the vapor diffusivity δ and (5) the vapor diffusion resistance μ.

Methods for determining the heat and mass transfer coefficients α and β or the thermal diffusivity λ are well known and considered as state of the art. Therefore, a more detailed analysis of these properties is not necessary, and it is suffice to simply refer to the relevant literature [3, 5–7].

On the other hand, the determination of the internal mass transfer coefficients, namely the moisture conductivity κ and the effective diffusion coefficient, which depends on the vapor diffusivity δ and the vapor diffusion resistance μ, is far more complicated. Experimental as well as theoretical methods for determining these transport coefficients are the subject of numerous studies [3, 8–10]. Unfortunately, in all instances it was established that the determination of the required quantities, either experimentally or theoretically, is a very time consuming and costly process and does not always yield the desired results.

However, since knowledge of these quantities is essential for the calculation of the heat and mass transfer rates, an efficient method in determining the required properties is presented in this paper. The moisture conductivity κ and vapor diffusion resistance μ are determined from the measurements of global properties and are calculated as local quantities by implementing a specifically developed inversion procedure.

As shown in Section 3, the procedure utilizes experimentally determined drying curves which illustrate the relationship between the extracted mass of water per unit time and the mean moisture content of the product. First of all, however, simple equations defining the moisture

conductivity, the vapor diffusivity and the vapor diffusion resistance are required.

2.2.1. Moisture conductivity

According to Härtling [11], the moisture conductivity κ is a multiple function of the product temperature and its moisture content. This function is described by a simple relation and can be expressed as a function of the local temperature ϑ and moisture content X,

$$\kappa = c_1 \left(\frac{\vartheta}{c_2}\right)^{c_3} \left(\frac{X}{c_4}\right)^{c_5} [\mathrm{m^2\ s^{-1}}]. \tag{18}$$

Determination of the dimensional parameters c_1 [$\mathrm{m^2\ s^{-1}}$] and c_2 [°C] and the dimensionless parameters c_3, c_4, c_5 which as weighing parameters reflect the dependence of the moisture content and the temperature, is based on the inversion procedure to be discussed in Section 3.

2.2.2. Vapor diffusivity and vapor diffusion resistance

As far as the vapor diffusivity δ and vapor diffusion resistance μ are concerned, matters are simplified by assuming that the diffusion term calculated by equation (10) takes a value other than zero only if a partial vapor pressure gradient exists within the substance. Especially, this is true after the substance has been greatly dehumidified causing formation of air filled pores which support the diffusion process. The shape and size of the pores change little during a continued dehumidification. In order to further avoid complications, the assumption is made, in accordance with Krischer and Kast [3], that an almost constant resistance is imposed on the diffusion flux as compared to the free diffusion of water vapor in air. Now, if the effective transport coefficient for diffusion is expressed as the ratio of the vapor diffusivity δ and the vapor diffusion resistance μ, which is dependent on the size and shape of the air filled pores, then the vapor diffusion resistance μ is more or less a constant. This assumption is verified by comparing the results of the simulation with experimentally determined drying curves at low product moistures, since for small moisture contents the diffusion process is viewed as the driving force for mass transfer.

For the temperature range of 20–90°C during the drying process, the vapor diffusivity δ is computed with Schirmer's empirical relationship [12],

$$\delta = \frac{22.6 \cdot 10^{-6}}{p\,[\mathrm{bar}]} \left(\frac{T}{273}\right)^{1.81} [\mathrm{m^2\ s^{-1}}]. \tag{19}$$

As illustrated by the above mentioned assumptions, the vapor diffusion resistance μ is approximated by a constant,

$$\mu = c \quad [-]. \tag{20}$$

The actual determination of the vapor diffusion resistance μ is made simultaneously with the calculation of the moisture conductivity κ, employing the inversion procedure described in Section 3.

2.3. Description of the numerical model

Since the set of partial differential equations for the moisture content and the temperature of the product derived in Subsection 2.1 cannot be solved analytically a numerical method has to be used. An explicit finite difference method is chosen as opposed to an implicit one, because the required quantities can be calculated immediately from the values of the preceding time step. Consequently, the governing equations are solved immediately while the numerical effort and the system inherent error of discretization is minimized.

For the numerical solution, the product is divided into $l_{\max}$ elements with the thickness Δr. All drying materials which can be modeled as either a sphere, cylinder or flat plate are taken into consideration. At time t the element l has a thickness Δr_l^t, the control surfaces A_l^t and A_{l+1}^t and a control volume V_l^t. For non-shrinking products these quantities are constant during the entire drying process. However, for products whose volume diminishes during the dehumidification process the following effects must be taken into account:

First of all, the volume reduction itself is determined by a suitable approach. One obvious choice is to express the volume as a function of the product moisture content. Effective approaches which are usually of an empirical nature are found in the appropriate literature for almost all products of interest. Decisive for the derivation is that the volume V_l^t of an element l with the specific moisture content X_l^t at the time t is expressed as a function of suitable input parameters. For example, one such relationship applicable for various substances is found in the publications of Fusco et al. [13] and Lorenzo et al. [14]. This approach allows for the representation of the volume V_l^t as a function of the initial volume $V_{0,l}$, the initial moisture content $X_{0,l}$ and the instantaneous moisture content X_l^t of the product. Thus, the general relationship for the momentary volume V_l^t is given by

$$V_l^t = V_l^t(V_{0,l}, X_{0,l}, X_l^t). \tag{21}$$

Inclusion of the volume reduction in the single solid model is difficult since at first the geometrical locations of the heat and mass transfer surfaces of the differential control volume elements are not known, implying that a boundary value problem with a moving boundary must be solved. Crank [15] introduces either the front-fixing method or the front-tracking method as a numerical scheme of these phenomena. The front-fixing method fixes the moving boundary by employing a coordinate transformation. Subsequently, the simplified boundary value problem is solved and the given result transformed back. Since the mathematical-numerical conversion of the method is extremely complicated, the front-tracking

method is used instead. It relies on the discrete adjustment of a grid fixed in space at for every time step Δt. Hence, for each time interval of the discretization of the differential equation the boundary is more or less fixed. This method in combination with a general relationship for the volume reduction as given by equation (21) enables the determination of the outer radius r_l^t, the control surface A_l^t and the thickness Δr_l^t of an element l as a function of the present moisture content X_l^t.

2.3.1. Finite difference equation for the product temperature and the moisture content

The partial differential equation for the product temperature [equation (7)] is transformed into a finite-difference equation by way of an explicit procedure. In order to determine the temperature distribution for the cross section of the substances the equation is solved for the product temperature $\vartheta_l^{t+\Delta t}$ at time $t+\Delta t$ for each element l. Considering that for a volume reduction the thickness of a spatial step is not constant but changes with time, then the temperature of the product at the time $t+\Delta t$ can be immediately calculated for all elements l from

$$\vartheta_l^{t+\Delta t} = \vartheta_l^t + \{\dot{Q}_{\lambda,l}^t - \dot{Q}_{\lambda,l-1}^t - [\dot{m}_{v,l}^t (h_{v,l+1/2}^t + h_{B,l+1/2}^t) - \dot{m}_{v,l-1}^t (h_{v,l-1/2}^t + h_{B,l-1/2}^t)]\} / \{\varrho_{sdr}(c_{sdr} + X_l^t c_w) V_l^t\} \cdot \Delta t. \tag{22}$$

Similar to the product temperature, the partial differential equation for the product moisture content [equation (9)] is converted into a finite difference equation and solved for $X_l^{t+\Delta t}$. This results in the governing equation for the product moisture content for all elements l at time $t+\Delta t$,

$$X_l^{t+\Delta t} = X_l^t - [\dot{m}_{f,l}^t + \dot{m}_{v,l}^t - (\dot{m}_{f,l-1}^t + \dot{m}_{v,l-1}^t)] / [\varrho_{sdr} V_l^t] \cdot \Delta t. \tag{23}$$

The finite-difference equations (22) and (23) require expressions for the finite heat conduction rate as well as for the finite mass transfer rates in the vapor and the liquid phase in finite-difference forms,

$$\dot{Q}_{\lambda,l}^t = -\lambda_{l+1/2} \cdot A_l^t \frac{\vartheta_{l+1}^t - \vartheta_l^t}{\Delta r_l^t} \tag{24}$$

$$\dot{m}_{v,l}^t = -A_l^t \left(\frac{\delta}{\mu} \frac{p_v^*}{R_v T} \left(\frac{\partial a_w}{\partial X} \right)_{l+1/2} \right) \cdot \frac{X_{l+1}^t - X_l^t}{\Delta r_l^t} \tag{25}$$

$$\dot{m}_{f,l}^t = -A_l^t (\varrho_{sdr} \kappa_{l+1/2}) \frac{X_{l+1}^t - X_l^t}{\Delta r_l^t}. \tag{26}$$

3. Inversion procedure

The main difficulty in dealing with mathematical models based on the fundamental conservation principles is the need for the transport properties contained in the governing equations. This is especially true for the experimentally hard to determine internal mass transfer coefficients. Since the applicability of the model is contingent on the effort required to obtain the necessary parameters, a theoretical approach in finding the transport properties is used. The objective now is to determine the *a priori* unknown internal mass transfer coefficients by means of easily obtained experimentally information.

Assuming that drying curves for almost every product are available in the pertinent literature and in data banks, respectively, or in the worst case can be determined without difficulty the obvious choice in specifying the internal mass transfer coefficients is by using drying curves as basic information. On this basis, a mathematical–numerical procedure is introduced enabling the determination of the local internal transport coefficients by way of various drying curves. The appropriate method utilizes the least square technique by Gauss [16]. Prerequisite for this technique is the availability of the transport properties as mathematical functions. Hereby, the values for the formal and at first unknown weighing parameters are changed by the inverse algorithm until the deviation between the experimentally determined drying curves and the simulated ones is minimized.

The difficulty with this optimization technique is not so much that the mathematical functions for the transport coefficients have to be correlated to measured values but rather that the output of the drying simulation has to be matched with empirical data.

3.1. Description of the algorithm

As described in Subsection 2.2 the moisture conductivity κ [equation (18)] and the vapor diffusion resistance μ [equation (20)] are defined formally with the help of weighing parameters. If these parameters are to be found by applying the least square technique then the mathematical independence of the parameters c_j must be guaranteed in order to obtain a converged solution. For this reason, the weighing parameters c_2 and c_4 in equation (18) initially have to be constant. Subsequently, the following two equations for the moisture conductivity κ and the vapor diffusion resistance μ are introduced as a function of the dimensionless parameters c_1, c_2, c_3, c_4, where k_1 [m^2 s^{-1}], k_2 [°C], k_3 [−] are assumed to be constants,

$$\kappa = c_1 \cdot k_1 \left(\frac{\vartheta}{k_2} \right)^{c_2} \cdot \left(\frac{X}{k_3} \right)^{c_3} \tag{27}$$

$$\mu = c_4. \tag{28}$$

The determination of the four unknowns coefficients c_j ($j = 1, \ldots, 4$) in equations (27) and (28) is only possible if at least two drying curves displaying the relationship between the loss of water mass per unit time and the

mean moisture content of the substance for steady conditions are on hand. Experimentally determined drying curves are denoted by y_i, and the computed drying curves by f_i, where $i = 1, \ldots, a0 \cdot n0$. Herein, $a0$ stands for the number of drying curves utilized and $n0$ for the number of data points per curve.

Considering that the number of unknown parameters c_j ($j = 1, \ldots, c0$) does not correspond to the number of governing equations $a0 \cdot n0$ (as a rule $n0 > 15$) but is substantially smaller, no unique and hence exact solution $(y_i - f_i) = 0$ exists. Therefore, if possible only an ideal solution, $(y_i - f_i) = \min$, is attainable, indicating that an optimization problem is on hand.

Such overdetermined sets of equations almost always lead to the least square technique given by Gauss at the beginning of the 19th century in connection with the analysis of planetary motion [16]. Gauss' method is not the only one available, but it has a number of advantages as is illustrated in this section. The objective is to choose the parameters c_j in such a way that the experimentally determined drying curves y_i match the computed curves f_i as closely as possible. This implies that the difference $(y_i - f_i)$ for all supporting points i ($i = 1, \ldots, a_0 \cdot n_0$) has to be minimized. For that purpose, the square function S is introduced [17],

$$S(c_1, \ldots, c_{c0}) := \|\mathbf{y} - \mathbf{f}\|^2 = \sum_{i=1}^{a0 \cdot n0} (y_i - f_i)^2 \tag{29}$$

with

$$\|\mathbf{y} - \mathbf{f}\|^2 := (\mathbf{y} - \mathbf{f})^T (\mathbf{y} - \mathbf{f}). \tag{30}$$

This equation represents the sum of the quadratic errors S to be minimized. Subjecting equation (29) to the theory of the relative extrema results in

$$\frac{\partial S}{\partial c_j} \overset{!}{=} 0 \quad j = 1, \ldots, c0. \tag{31}$$

Now, if f is differentiable, equation (29) becomes a basic equation for the evaluation of the undetermined parameters $c_1, \ldots, c_{c0}$,

$$\frac{\partial S}{\partial c_j} = 2 \sum_{i=1}^{a0 \cdot n0} (y_i - f_i) \cdot \left(- \frac{\partial f_i}{\partial c_j} \right) \overset{!}{=} 0. \tag{32}$$

The preceding expression results in a number of equations $c0$ with an equal number of unknowns. If the partial derivative $\partial f_i / \partial c_j$ can be determined, then the required parameter c_j can be computed from the given set of equations. A considerable advantage is that as the sum of squared values the function S [equation (29)] possesses only one extremum, namely, a minimum. In addition, it is possible to weigh single measurements by multiplying the set of equations with a weighing matrix. A disadvantage, however, is the nonlinear dependence on the measurement errors so that greater deviations lead to an overrating. Therefore, it is desirable to delete obviously incorrect data points before starting the optimization procedure [16].

Since the partial derivative $\partial f_i / \partial c_j$ cannot be formed directly, the set of equations (32) in its present form cannot be used to determine the parameters. Instead, some transformations are necessary:

Vector notation is employed, whereby equation (29) becomes

$$\begin{aligned} \frac{\partial}{\partial c_j} S &= \frac{\partial}{\partial c_j} \|\mathbf{y} - \mathbf{f}\|^2 \\ &= \mathbf{grad}_c \|\mathbf{y} - \mathbf{f}\|^2 \overset{!}{=} 0 \end{aligned} \tag{33}$$

with

$$\mathbf{grad}_c = \left(\frac{\partial}{\partial c_1}, \ldots, \frac{\partial}{\partial c_{c0}} \right).$$

The next step is to linearize f using the Taylor series around the developing vector $\mathbf{c}'$. Assuming that the starting conditions denoted by vector $\mathbf{c}$ closely match the best possible solution $\mathbf{c}'$, then the linear terms of the Taylor series have to be considered

$$f(\mathbf{c}) = f(\mathbf{c}') + \frac{\partial f}{\partial c_1} \Delta c_1 + \cdots + \frac{\partial f}{\partial c_{c0}} \Delta c_{c0}, \tag{34}$$

with

$$\Delta \mathbf{c} = \mathbf{c} - \mathbf{c}'. \tag{35}$$

Now, the linearized inverse problem based on the given number of curves a_0 and the supporting data points n_0 becomes,

$$\begin{aligned} &\begin{bmatrix} f_1(\mathbf{c}) \\ \vdots \\ f_{a0 \cdot n0}(\mathbf{c}) \end{bmatrix} \\ &= \begin{bmatrix} f_1(\mathbf{c}') + \dfrac{\partial f_1}{\partial c_1} \Delta c_1 + \cdots + \dfrac{\partial f_1}{\partial c_{c0}} \Delta c_{c0} \\ \vdots \\ f_{a0 \cdot n0}(\mathbf{c}') + \dfrac{\partial f_{a0 \cdot n0}}{\partial c_1} \Delta c_1 + \cdots + \dfrac{\partial f_{a0 \cdot n0}}{\partial c_{c0}} \Delta c_{c0} \end{bmatrix} \\ &= \mathbf{f} + \mathbf{A}\, \Delta \mathbf{c}. \end{aligned} \tag{36}$$

To enable numerical handling of the matrix $\mathbf{A}$ (i.e., once again it is emphasized that f is not a mathematical function but represents a complete drying simulation procedure), the differential-quotients are substituted by difference-quotients, whereby Δc_j has to be sufficiently small so that

$$\begin{aligned} \mathbf{A} &= \left(\frac{\partial f_i}{\partial c_j} \right) \\ &= \left(\frac{f_i(\ldots, c_j + \Delta c_j, \ldots) - f_i(\ldots, c_j \ldots)}{\Delta c_j} \right). \end{aligned} \tag{37}$$

Implementing this relation in equation (33) leads to

$$\mathbf{grad}_{\mathbf{c}}\|\mathbf{y}-\mathbf{f}\|^2 = \mathbf{grad}_{\Delta c}\|\mathbf{y}-\mathbf{f}-\mathbf{A}\,\Delta\mathbf{c}\|^2 \stackrel{!}{=} \mathbf{0}.$$

Finally, the resulting matrix equation is

$$\mathbf{A}^T\mathbf{A}\,\Delta c = \mathbf{A}^T(\mathbf{y}-\mathbf{f}) \tag{38}$$

with a square coefficient matrix $c_{c0} \times c_{c0}$ and a corresponding solution vector, In general, unambiguous results are found for the vector $\Delta\mathbf{c} = \mathbf{c}-\mathbf{c}'$, where $\mathbf{c}'$ is a better estimate for the parameters c_j contained in vector $\mathbf{c}$. The procedure is repeated until the difference (y_i-f_i) or rather the vector $\Delta\mathbf{c}$ is small enough and satisfies the criterion for terminating the optimization process. With respect to the numerical implementation employed in the course of the study, reference is made to the dissertation [1] for the details.

3.2. Application for the algorithm

For easier understanding of the procedure used in determining the transport properties an operational oriented description of the inversion procedure follows for concrete as an example. Values adapted are those for the moisture conductivity κ and the vapor diffusion resistance μ.

As has already been mentioned the parameters c_1, c_2, c_3, c_4 in equations (27) and (28) have to be determined to such an extent that the simulated drying curves f_i coincide with the experimentally obtained drying curves y_i. Now, the main difficulty in applying this novel procedure is in selecting the appropriate initial values for the requirement parameters. As far as the moisture conductivity κ is concerned this is accomplished by either regarding the theoretical models available [1] or by strictly applying the inversion procedure. A first approximation for c_4 which stands for the vapor diffusion resistance μ is chosen from the experimental data available in the literature. In addition, values for the constants k_1, k_2 and k_3 in equation (27) for the moisture conductivity κ must be determined. It should be noted that for numerical reasons the values of k_j cannot be changed simultaneously with the weighing parameters c_j. Prior simulation runs have shown that the values $k_1 = (1/3600)$ [m^2 s^{-1}], $k_2 = 273$ [°C] and $k_3 = 0.6$ [−] provide good results for the tested materials such as concrete, brick, clay, wheat and pine.

The inversion numerical method requires that the initial values lie within a correct order of magnitude. As is shown elsewhere [1], materials with a similar structure also possess similar transport properties. Thus, the inversion procedure for an unknown material can be started by substituting initial values for the undetermined parameters of a similar substance with known properties.

By means of three drying curves of concrete measured by Härtling [11] under different drying conditions (listed in Table 1), the step-by-step inversion procedure for the determination of the moisture conductivity and the vapor diffusion resistance are illustrated in Figs. 1–3. Computed drying curves are shown as lines and experimental data are given by symbols. Initial values for c_1, c_2 and c_3 were found after a few test runs. The starting value for $\mu = c_4 = 10$ is the mean average value calculated from the values available in the literature.

Figure 1 displays the first iteration step for three simulations of drying curves subjected to different drying conditions. The initial values of the inversion parameters c_j are given in the legend. Figure 2 contains the fifth and Fig. 3 the tenth iteration steps together with the adapted weighting parameters. Convergence is achieved by modifying the parameters by the inversion procedure. By comparing the computed and the experimental drying

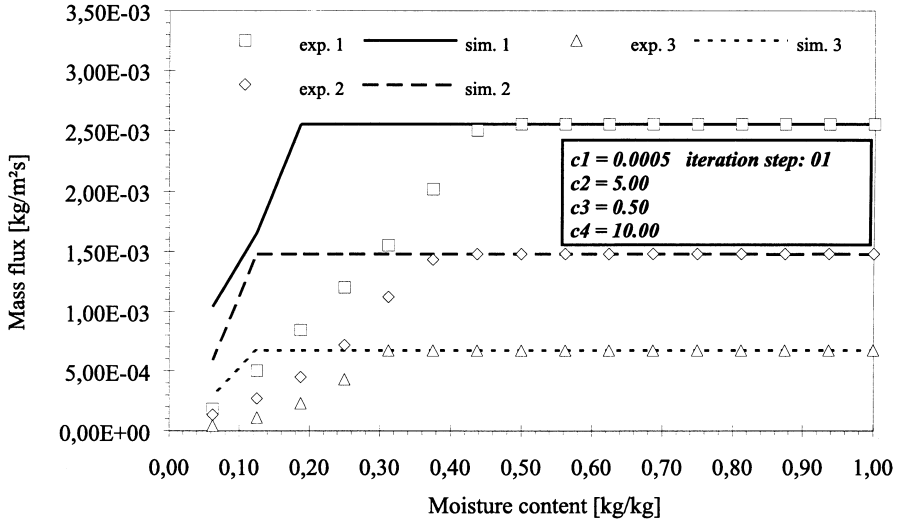

Fig. 1. Step 01 of the inversion procedure.

Table 1
Drying conditions for the inversion procedure

Exp.	Source	ϑ_a [°C]	x_a [g kg^{-1}]	w_a [m s^{-1}]	d [m]	Material
1	[11]	156.7	3.8	4.8	0.0405	Concrete-sphere
2	[11]	98.3	7.7	4.9		
3	[11]	52.5	7.4	5.0		

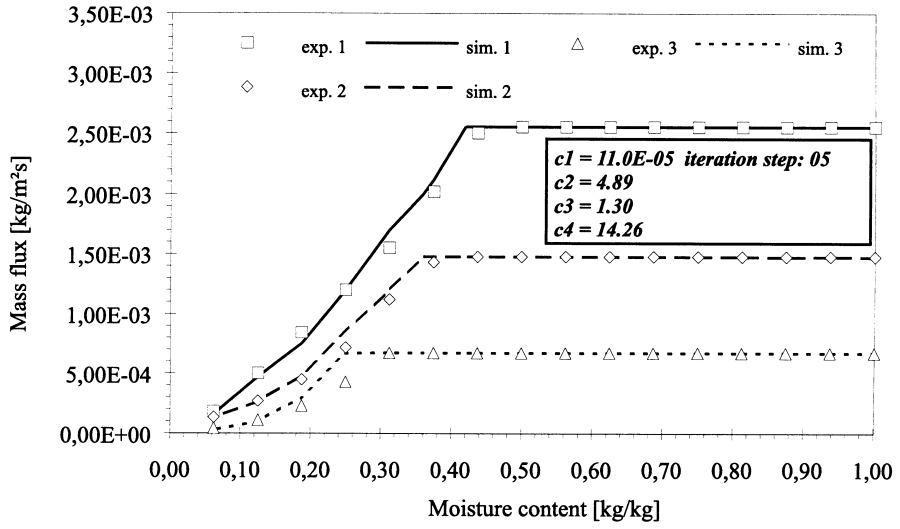

Fig. 2. Step 05 of the inversion procedure.

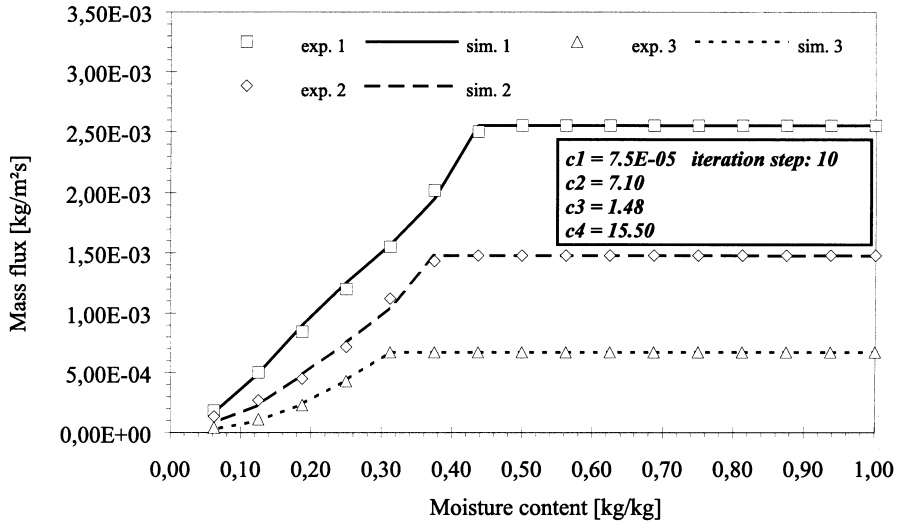

Fig. 3. Step 10 of the inversion procedure.

Table 2
Results of the inversion process

	$\kappa = (c_1/3600)(\vartheta/273\,[^\circ C])^{c_2}(X/0.6)^{c_3}$ [m^2 s^{-1}]			$\mu = c_4$ [−]	Range of validity	
	c_1	c_2	c_3	c_4	ϑ [°C]	X [kg kg^{-1}]
Concrete	$7.5 \cdot 10^{-5}$	7.10	1.48	15.5	30 ... 150	⩽1.00
Brick	$3.6 \cdot 10^{-5}$	9.41	0.84	6.4	30 ... 150	⩽0.30
Clay	$5.7 \cdot 10^{-5}$	6.18	0.72	15.0	30 ... 150	⩽0.25
Wheat	$2.5 \cdot 10^{-8}$	1.23	0.15	150.0	30 ... 100	⩽0.32
Pine	$1.13 \cdot 10^{-6}$	5.03	0.60	99.5	30 ... 70	⩽0.35

curves it is obvious that after only ten iterative steps both curves display an almost identical behavior, implying that the determination of the undetermined parameters is sufficiently exact. The criterion for terminating the procedure was set at $\Delta \mathbf{c} < 10^{-5}$. Following this approach, the required transport coefficients κ and μ for concrete, brick, clay wheat and pine were determined [1]. Values for the various weighing parameters as well as the range of validity are summarized in Table 2.

4. Verification of the computational model

The selection of materials for the verification of the (single solid) simulation model was based on the following consideration. By choosing materials which differ in hygroscopicity, volume contraction and geometry the validity of the model for simulating the drying behavior of single solids is demonstrated for a broad spectrum of materials exhibiting a capillary porous inner structure and hygroscopic features. Taking the above mentioned aspects into account, the materials used for the validation of the single solid model are concrete, brick, clay, wheat and pine [1].

4.1. Drying under time constant conditions

Here, the drying curves of concrete and pine obtained experimentally under time independent conditions are compared with drying curves calculated numerically for the same externally imposed conditions employing the single solid model. In Table 3 the conditions are listed under which the experiments were performed as well as the geometries of the substances examined. For each experiment the drying conditions are specified by the temperature ϑ_a, the moisture content x_a and the velocity w_a of the drying medium (air). The dimension d represents the diameter of the substance or in the case of a flat plate its thickness. In most instances, the drying process is illustrated in the form of drying curves which show the specific drying rate as mass flux over the mean moisture content of the product. In the figures the simulated runs are identified by lines and the experimentally determined ones by symbols.

First of all, it is shown that the single solid model accurately describes the drying behavior of solids with different geometries. For this reason experimental drying curves of concrete structured as a sphere, cylinder and plate are compared to predicted curves in Figs. 4–6. The curves substantiate the near perfect matching of the simulation data with the experimental results, thus confirming the ability of the model to correctly describe the drying behavior of materials with different geometries.

Figures 4–6 indicate that at the beginning of the drying process the drying curves for concrete display a section of constant drying rate for the stated drying conditions. This effect, which the literature designates as the first drying period, takes place as long as the moisture content at the surface of the product is larger than the corresponding maximum hygroscopic moisture content. The pronounced seemingly steady state condition exists only if the product moisture content is very high compared to the maximum hygroscopic moisture content at the beginning of the drying process.

Using pine as an example in Fig. 7, it is shown that the drying of a material having a totally different drying behavior due to varying inner structures can also be predicted with the simulation model. The reason for the absence of a first drying period for pine (Fig. 7) is explained by the fact that for this substance the moisture content at the beginning of the drying process is in the vicinity of the maximum hygroscopic moisture content, and consequently the seemingly steady state condition cannot develop.

Moreover, it is demonstrated [1] that the moisture and temperature distribution for the cross section of the product can be closely modeled in the same way as the mean moisture content.

Figure 8 emphasizes the efficacy of the inversion procedure for determining the internal mass transfer coefficients: namely, if two experimentally determined drying curves are available, then the inversion procedure yields the moisture conductivity and the vapor diffusion resistance for the subsequent simulation of the curves 1

Table 3
Drying conditions

Experiment	Source	ϑ_a [°C]	x_a [g kg^{-1}]	w_a [m s^{-1}]	d [m]	Substance
1	[11]	156.7	3.8	4.8	0.0405	Concrete-sphere
2	[11]	98.3	7.7	4.9		
3	[11]	52.5	7.4	5.0		
4	[11]	103.1	3.7	4.9	0.0095	Concrete-plate
5	[11]	53.3	4.8	4.9		
6	[11]	99.4	6.6	4.8	0.0300	Concrete-cylinder
7	[11]	50.2	10.4	4.9		
14	[1]	70.0	113.2	3.0	0.025	Pine-plate
15	[1]	50.0	31.9	3.0		

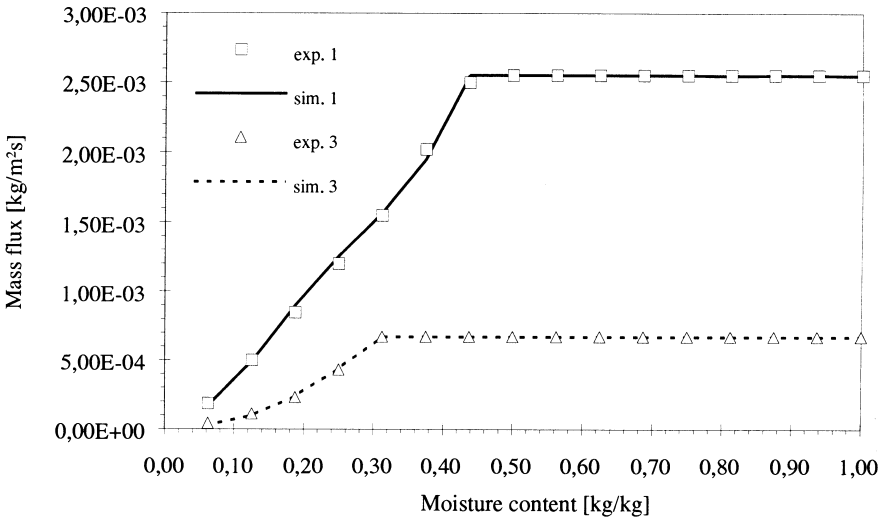

Fig. 4. Drying of a concrete-sphere in air.

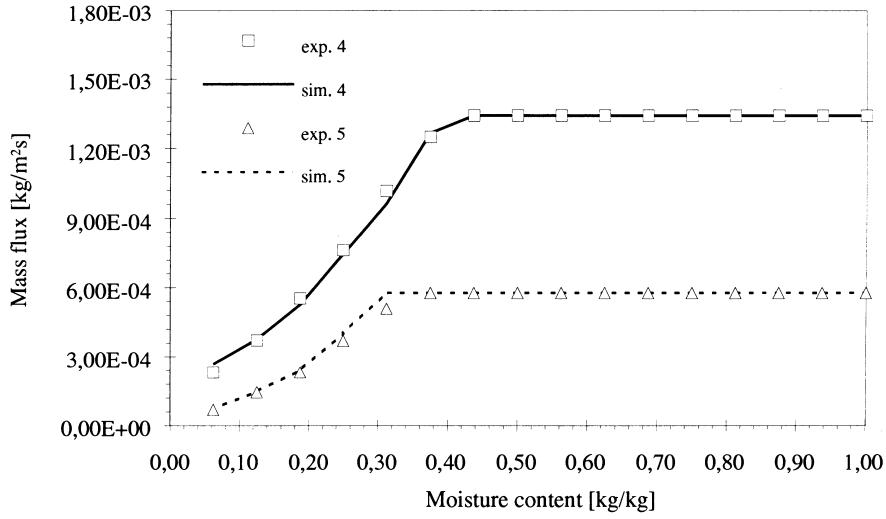

Fig. 5. Drying of a concrete-plate in air.

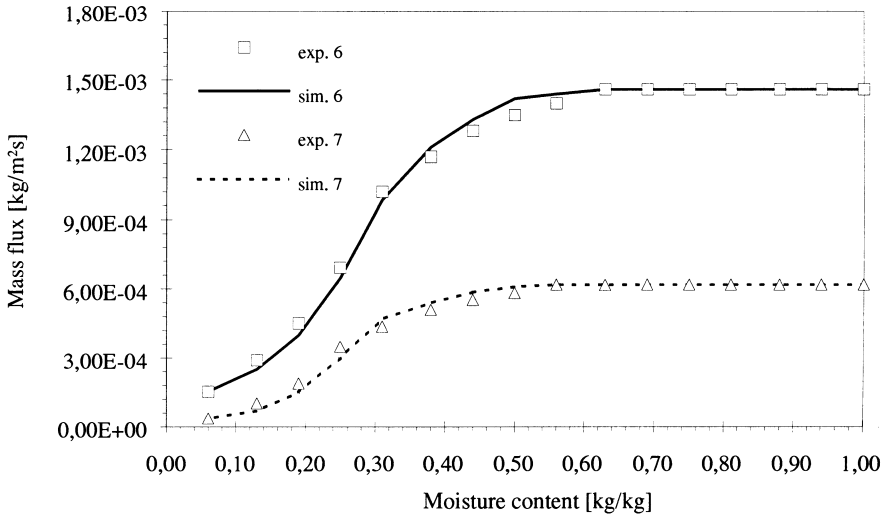

Fig. 6. Drying of a concrete-cylinder in air.

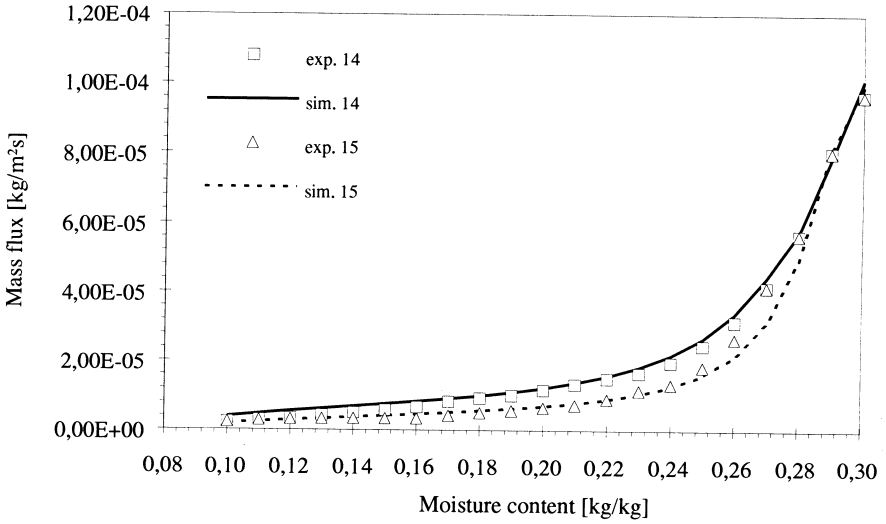

Fig. 7. Drying of a pine-plate in air.

and 3 in Fig. 8. With these transport coefficients, additional curves can readily be computed, for example, curve 2. The excellent agreement with the experimental data is proof for the quality of the novel technique.

4.2. Drying under time dependent conditions

In order to answer the question whether the single solid model accurately describes the drying behavior not only for time independent but also for time variable drying conditions, once again experimentally obtained data are compared with predicted results of simulated drying processes. The drying conditions are in accordance with the states of the drying medium air that prevail after the air has been heated in a solar collector. Thus, the air temperature varies between 17 and 59°C, and the absolute air humidity between 9 and 42 g kg^{-1} as shown in Fig. 9. These time dependent drying conditions impose stringent requirements on the simulation model. Because of the minor influence of the velocity of the drying medium on the actual drying behavior, the flow rate is fixed at 3 m s^{-1} and held constant for the entire experiment.

In Figs. 10 and 11 the experimentally determined curves of the mean product temperature and the moisture

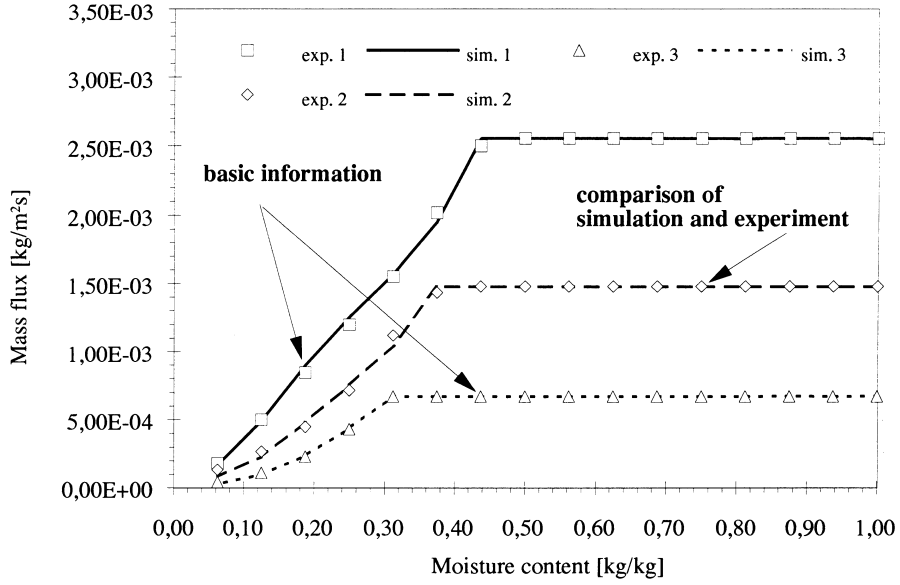

Fig. 8. Efficacy of the inversion procedure.

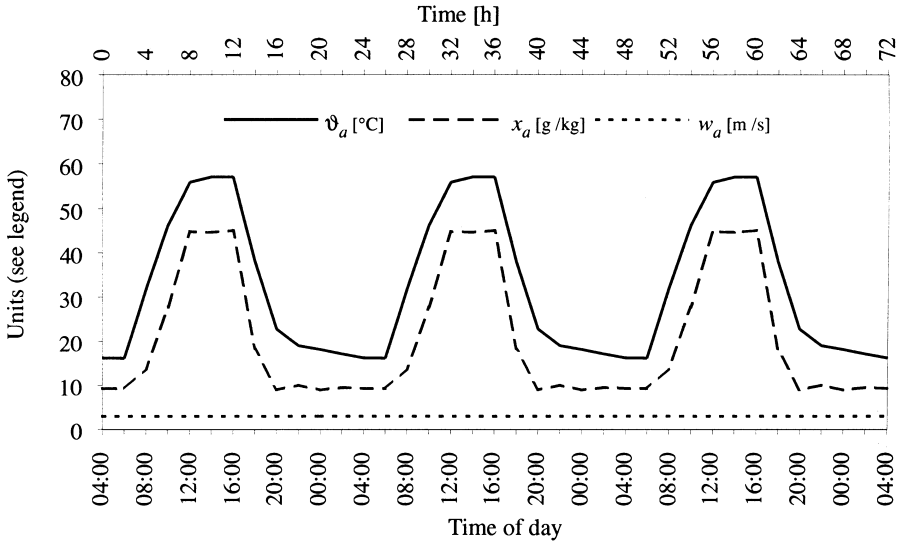

Fig. 9. Drying conditions over time.

content over the drying time are compared with the results of the simulation. The figures illustrate the drying features of a 2.5 cm thick slab of pine for the drying conditions given in Fig. 9.

Despite the fact that the predicted values are slightly higher than the measured ones a good match of the experimental results with the simulated ones is apparent. Deviations of the moisture content in the experiment and simulation occur mainly for very small mean temperatures, because the internal mass transfer coefficients are not verified for temperatures below 30°C as indicated in Table 2. Still, even for low temperatures useful results are obtained, which underlines the possibility of extrapolating the internal mass transfer coefficients determined with the inversion procedure. Consequently the novel single-solid simulation model correctly describes

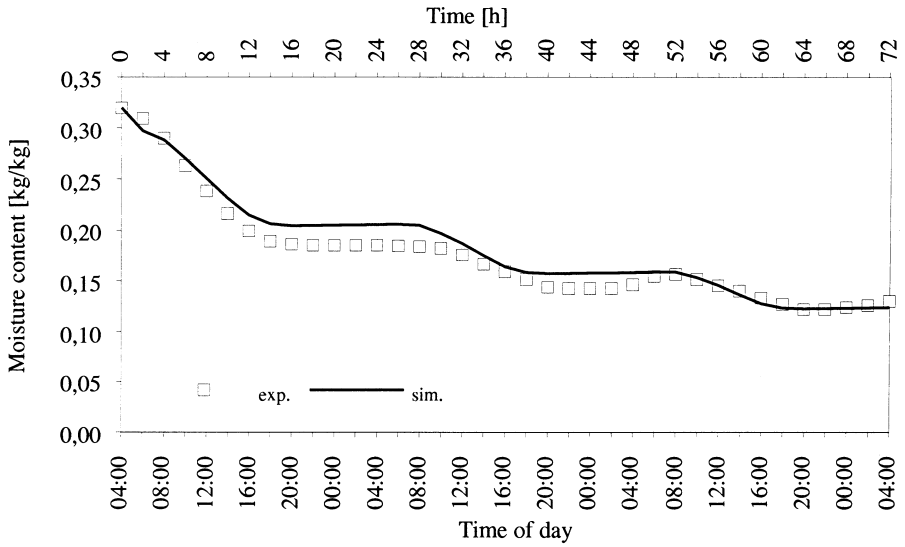

Fig. 10. Drying of a pine-plate—mean moisture content over time.

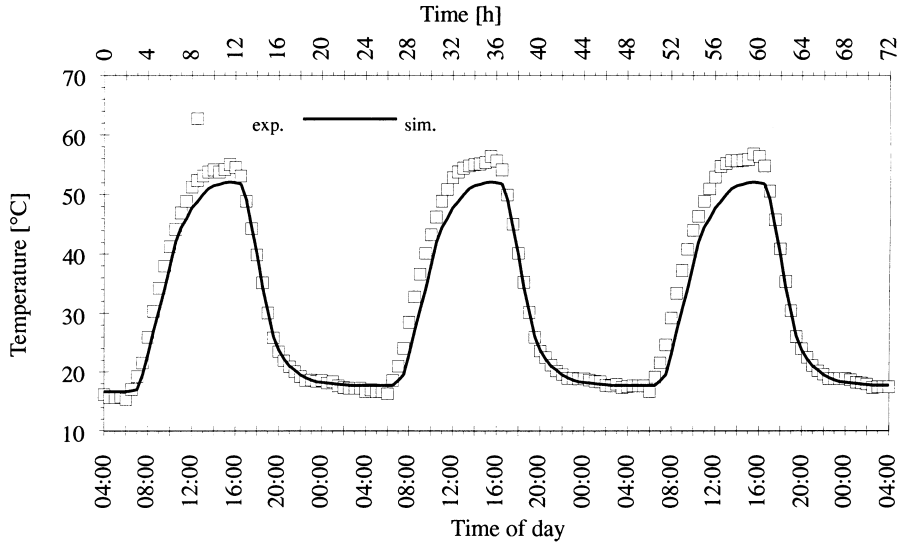

Fig. 11. Drying of a pine-plate—mean product temperature over time.

the drying behavior of capillary porous, hygroscopic substances under time dependent drying conditions.

The verification of the ability of the single solid model to predict the drying behavior for time dependent drying conditions is an important requirement, especially for the description of the drying of packed beds. This is because at different depths within the packed bed the single solids are subjected to every changing drying conditions due to the moisture increase and thus changing temperatures of the drying medium air.

5. Conclusions

Based upon the fundamental principles of heat and mass transfer a physical-mathematical and a numerical

model describing the drying of a single solid was developed. This single solid model forms the basis for development of a further model simulation the drying features of packed beds which is discussed in the dissertation [1] and will be published in a separate paper.

The single solid model is based on the conservation of heat and enthalpy flow rates as well as mass flow rates for a differential control volume. With regard to the mass transfer a distinction is made between mass transfer in the liquid phase and in the vapor phase. This approach results in a set of combined partial differential equations for the temperature and moisture content of the drying substance. The model equations can be solved numerically if the transport coefficients are known and the prevailing boundary conditions are taken into account. Equations for all properties, states of equilibrium and transport coefficients contained in the model are found in the relevant literature. Two exceptions are the moisture conductivity and the vapor diffusion resistance. By definition, these two internal mass transfer coefficients are closely linked to the single solid model implying that their values cannot be taken from the literature. Therefore, an inversion procedure was developed which allows the determination of the two unknown transport properties by utilizing experimentally obtained drying curves. This procedure requires at least two different experimentally determined drying curves.

The computer program implementing the single solid model and the inversion procedure for determining the a priori unknown internal transfer coefficients allows for a reliable prediction of the drying behavior of capillary porous, hygroscopic solids under time constant and time dependent drying conditions. A comparison of results of simulations and experiments obtained for concrete, brick, clay, wheat and pine, which differ with respect to hygroscopicity, volume contraction and geometry proves the efficacy of the novel computational tool for the simulation and optimization of drying processes.

References

[1] Dietl C. Numerische und experimentelle Untersuchungen zum Trocknungsverhalten kapillarporöser, hygroskopischer Stoffe, Fortschr.-Ber., Reihe 3, Nr. 393. Düsseldorf: VDI, 1995.
[2] Luikov AV. Systems of differential equations of heat and mass transfer in capillary porous bodies. Int J Heat 1975;18:1–14.
[3] Krischer O, Kast W. Die wissenschaftlichen Grundlagen der Trocknungstechnik. Berlin: Springer, 1978.
[4] Jokisch F. Über den Stofftransport im hygroskopischen Feuchtebereich kapillarporöser Stoffe am Beispiel des Wasserdampftransports in technischen Adsorbentien. Dissertation, TH Darmstadt, 1974.
[5] Kast W, Krischer O, Reinicke H, Wintermantel K. Konvektive Wärmeund Stoffübertragung. Berlin: Springer, 1974.
[6] Gnielinski V. Berechnung mittlerer Wärme- und Stoffübergangskoeffizienten an laminar und turbulent überströmten Einzelkörpern mit Hilfe einer einheitlichen Gleichung, Sonderdruck aus Forsch.-Ing.-Wes 1975;41.
[7] Kostaropoulus AF, Wolf W, Spiess, WEL. Modelle für die theoretische Bestimmung der Wämeleitzahl inhomogener poröser Stoffe. Lebnsm Wiss u Technol 1975;8:177–180.
[8] Neiß J. Numerische Simulation des Wärme- und Feuchtetransports und der Eisbildung in Böden, Fortschr.-Ber., Reihe 3, Nr. 73. Düsseldorf: VDI, 1982.
[9] Schubert H. Kapillarität in porösen Feststoffsystemen. Berlin: Springer, 1982.
[10] Kießl K. Kapillarer und dampfförmiger Feuchtetransport in mehrschichtigen Bauteilen, Dissertation, Universität Essen, 1983.
[11] Härtling M. Messung und Analyse von Trocknungsverlaufskurven als Grundlage zur Vorausberechnung von Trocknungsprozessen, Dissertation, TH Karlsruhe, 1978.
[12] Schirmer R. Die Diffusionszahl von Wasserdampf-Luftgemischen und die Verdampfungsgeschwindigkeit, Beiheft Verfahrenstechnik, Nr. 170. Düsseldorf: VDI, 1938.
[13] Fusco AJ, Avarez JR, Aguerre RJ, Gabitto JF. A diffusional model for drying with volumetric change. Drying Technology 1978;9(2):207–12.
[14] Lozano JE, Rotstein E, Urbicain MJ. Shrinkage, porosity and bulk density of foodstuffs at changing moisture contents, J Food Sci 1983;48:1497–502, 1553.
[15] Crank J. Free and Moving Boundary Problems. Oxford: Clarendon, 1984.
[16] Papageorgiou M. Optimierung. München: Oldenburg, 1991.
[17] Bronstein JN, Semendjajew KA. Taschenbuch der Mathematik. Thun: Harri Deutsch, 1984.